

Enhancing Effect of SiO_x Monolayer Coverage of TiO₂ on the Photoinduced Oxidation of Rhodamine 6G in Aqueous Media

Hiroaki Tada,*[†] Manabu Akazawa,[‡] Yasuyuki Kubo,[‡] and Seishiro Ito[‡]

Environmental Science Research Institute, Kinki University, 3-4-1, Kowakae, Higashi-Osaka, 577-8502, Japan, and Department of Applied Chemistry, Faculty of Science and Engineering, Kinki University, 3-4-1, Kowakae, Higashi-Osaka, 577-8502, Japan

Received: January 27, 1998; In Final Form: April 20, 1998

The effect of coating TiO₂ with a SiO_x monolayer on the photoinduced oxidation of rhodamine 6G (R-6G, counteranion X = Cl[−], NO₃[−]) has been studied. The surface treatment increased 2.6-fold the saturated adsorption amount (Γ_s) and 2.6-fold the adsorption strength (β) of R-6G⁺ ions. The rate of the liquid-phase oxidation was found to be dependent on X and increased remarkably with the SiO_x monolayer coating, in contrast to its inhibitive effect in the gas-phase oxidation. A modified Langmuir–Hinshelwood mechanism, where the reaction rate is assumed to be proportional to the coverage of the R-6G⁺ ion determined by the balance between the adsorption rate and the decomposition rate at the photostationary state, was proposed. As a result of kinetic analyses, the promoting effect in the liquid-phase oxidation was attributable to the increases in β , Γ_s , and/or the decrease in the adsorption amount of counteranions, which cannot be realized in the gas-phase reaction.

Introduction

The possibility of the application to water decontamination has driven many researchers to develop semiconductor photocatalysts.¹ TiO₂ is believed to be the best material for that purpose at present because of its powerful oxidation strength, high photostability in water, and nontoxicity. The essential object to be achieved is the increase of the efficiency of the photocatalytic oxidation.² In principle, the photocatalytic oxidation of organics is induced by holes (h⁺) generated in the valence band (VB) of TiO₂ upon the band gap excitation. It has been established in many reaction systems that heterogeneous photocatalytic oxidation obeys the Langmuir–Hinshelwood (LH) mechanism.³ This means that the degradation proceeds via quasi-bimolecular reaction between organic compounds adsorbed and charge carriers (or surface trapped carriers) on the surface. Two strategies can be envisaged in order to increase the reaction efficiency per unit surface area. The first is to increase the rate of charge transport to the surface at the photostationary state; this is chiefly associated with bulk properties of TiO₂ such as high crystallinity and purity.⁴ The second is to increase the adsorption rate of organic substrates at the photostationary state. Especially in practical dilute reaction systems, the second factor becomes of more importance. However, photocatalysts capable of increasing the adsorption rate are not present except for the materials comprised of TiO₂ and adsorbents, whose activities per unit weight are inevitably decreased.⁵

SiO_x monolayers are formed on the surface of TiO₂ by a method consisting of chemisorption of 1,3,5,7-tetramethylcyclotetrasiloxane (TMCTS) and subsequent irradiation ($\lambda > 300$ nm).⁶ The preceding paper reported that the rate of TiO₂

photoinduced oxidation of a cationic surfactant, cetylpyridinium bromide (CPB), in aqueous solution is increased with the SiO_x monolayer coverage.⁷ It was suggested that the increase in the rate of adsorption due to the electrostatic attraction between the parent surfactant ion (CP⁺) and the surface (Si_s–O[−]) is responsible for the finding. This paper describes a remarkable enhancing effect of the SiO_x monolayer coverage on the TiO₂ photoinduced oxidation of a cationic dye, rhodamine 6G (R-6G). Particular emphasis was placed on the kinetic analyses to clarify the origin of the effect.

Experimental Section

1,3,5,7-Tetramethylcyclotetrasiloxane (200 mL) (TMCTS, >98% pure, Shin-Etsu Chemical Co.) was allowed to react with 2 g of TiO₂ particles (A-100, Ishihara Sangyo Co., anatase, average particle diameter = 0.15 μ m, BET surface area = 8.1 m² g^{−1}) placed in a vacuum chamber under 0.6 \pm 0.1 Torr at 80 $^{\circ}$ C for 0.5 h. Then the temperature was raised to 100 $^{\circ}$ C, and evacuation continued for an additional 0.5 h to remove the physisorbed TMCTS. After the particles obtained (TMCTS/TiO₂) had been floated on the surface of 100 mL of aerated H₂O, they were irradiated under magnetic stirring with a 400 W high-pressure mercury arc (H-400P, Toshiba). The light intensity integrated between 320 and 400 nm impinging on the sample corresponds to an energy flux of 8.0 mW cm^{−2} ($I_{320-400}$). Upon irradiation, the particles began to sink because of the oxidation of hydrophobic Si–CH₃ groups of chemisorbed TMCTS to hydrophilic Si–OH groups. When irradiation was continued for 1 h, the particles were completely dispersed into the solution. Then the particles were recovered with centrifugation (rotation speed = 12 000 rpm) and dried in a vacuum desiccator at room temperature (SiO_x/TiO₂, BET surface area = 6.8 m² g^{−1}).

Rates of TiO₂ (or SiO_x/TiO₂) photoinduced decomposition of R-6G (reagent grade, >97% pure, Kanto Chemicals) were determined directly with R-6G solutions having various con-

* To whom correspondence should be addressed. Telephone: +81-6-721-2332. Fax: +81-6-721-3384. E-mail: h-tada@apsrv.apch.kindai.ac.jp.

[†] Environmental Science Research Institute.

[‡] Department of Applied Chemistry.

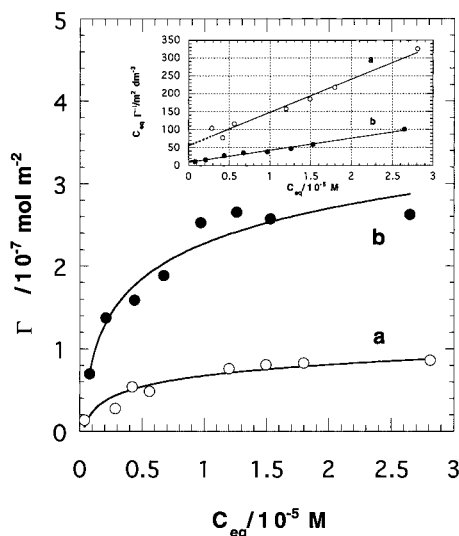


Figure 1. Adsorption isotherms of R-6G from aqueous solutions on TiO_2 (a) and $\text{SiO}_x/\text{TiO}_2$ (b) particles at $25 \pm 0.1^\circ\text{C}$ ($\text{pH} = 5.7$). C_{eq} was measured after 2 h. Catalyst concentration was fixed at 1 g/L. The inset is the Langmuir plots for TiO_2 (a) and $\text{SiO}_x/\text{TiO}_2$ (b) systems.

centrations at $21 \pm 1^\circ\text{C}$ (initial $\text{pH} = 5.7$). A slurry of 50 mL of distilled H_2O (air-saturated) and 0.05 g of catalyst was prepared in a photochemical reaction vessel made of Pyrex glass. Steady-state irradiations were carried out using the same ultraviolet (UV) light source as in the preparation of $\text{SiO}_x/\text{TiO}_2$ ($I_{320-400} = 1.2 \text{ mW cm}^{-2}$). A 300 W Xe lamp (Wacom, model XDS-301S) was used for visible (vis) light illumination ($\lambda > 420 \text{ nm}$, $I_{420-480} = 2.2 \text{ mW cm}^{-2}$). Aliquots of 10 mL were periodically removed and centrifuged, and the concentration of R-6G was determined from the absorbance of the peak maximum at 527 nm ($\epsilon_{\text{max}} = 8.09 \times 10^4 \text{ M}^{-1} \text{ cm}^{-1}$) on a Hitachi U-400 spectrophotometer. Adsorption isotherms were obtained in a similar way by exposing the catalysts to solutions with different concentrations of R-6G in the absence of irradiation followed by centrifugation and spectrophotometric analysis of R-6G remaining in the solutions. The Cl^- counteranion of R-6G^+ was exchanged into NO_3^- using an anion-exchange resin (DOWEX 1-X8). An amount of 80 g of the anion-exchange resin pretreated with a 4 wt % NaOH solution was added to 0.4 L of a R-6G solution ($6 \times 10^{-5} \text{ M}$, $\text{pH} = 5.7$) and stirred for 24 h. The resin was separated from the solution by filtration. The same procedures were repeated three times so that free Cl^- ions could not be detected in the filtrate by adding a AgNO_3 solution. Finally, the pH of the filtrate ($\text{pH} = 9.8$) was controlled at 5.1 with a dilute HNO_3 solution.

In gas-phase reactions, different amounts of R-6G were preadsorbed on the photocatalysts as follows. An amount of 0.1 g of photocatalysts was dispersed into 100 mL of R-6G solutions with varying concentrations ($1 \times 10^{-6} < C < 6 \times 10^{-6} \text{ M}$) and stirred for 24 h at 25°C . The particles were recovered by centrifugation (rotation speed = 12 000 rpm). After evaporation, the residual water was removed by drying in a vacuum desiccator at room temperature for more than 24 h. The particles adsorbed with R-6G in the air were irradiated with UV light ($\lambda > 300 \text{ nm}$, $I_{320-400} = 3.1 \text{ mW cm}^{-2}$). From the variation of the absorbance at 527.5 nm determined from the diffuse reflectance method using the UV-vis spectrophotometer, the rate constant of the gas-phase decomposition of R-6G was obtained by applying the first-order rate equation.^{5b,6b}

The energy eigenvalues of the R-6G^+ ion were obtained by the PM3 molecular orbital (MO) calculations. A newer MO model, PM3, is a modification of Dewar et al.'s improved

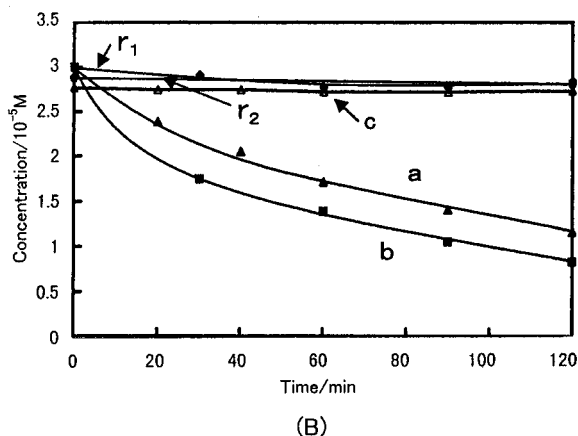
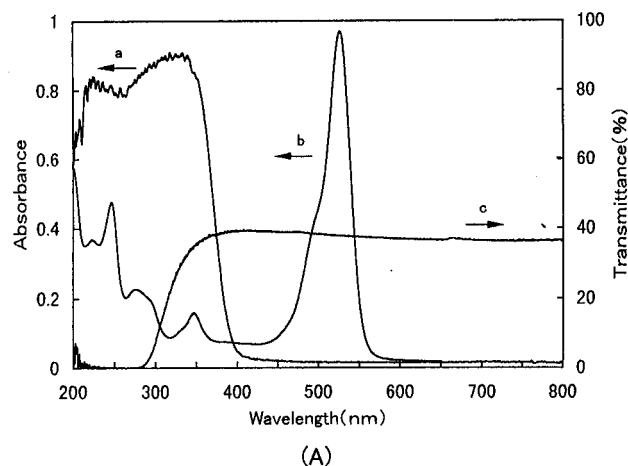


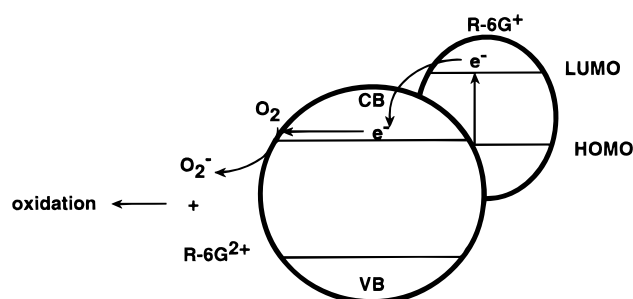
Figure 2. (A) Electronic absorption spectra of TiO_2 (a) and R-6G (b); the transmission spectrum of Pyrex glass (c). (B) Time courses of the photoinduced degradation of R-6G: $\lambda > 300 \text{ nm}$ irradiation without photocatalysts (r_1); dark reaction in the presence of TiO_2 (r_2); $\lambda > 300 \text{ nm}$ irradiation in the presence of TiO_2 (a) and $\text{SiO}_x/\text{TiO}_2$ (b); $\lambda > 420 \text{ nm}$ irradiation in the presence of TiO_2 (c). In these experiments, irradiation was started after reaching the adsorption equilibrium for each system.

version of MNDO, termed AM1.⁸ The energy eigenvalues for the optimized structure were calculated within MOPAC, version 5.0, with the PM3 method, where the H_2O solvent effect was taken into account by the conductor-like screening method.

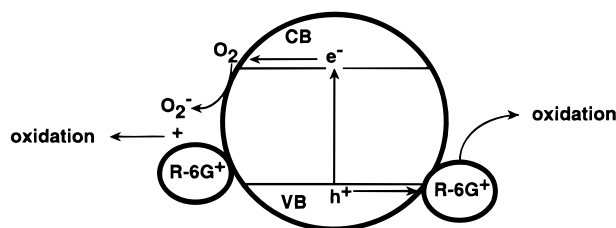
Results and Discussion

Figure 1 shows adsorption isotherms of R-6G from aqueous solutions on TiO_2 (a) and $\text{SiO}_x/\text{TiO}_2$ (b) particles at $25 \pm 0.1^\circ\text{C}$ ($\text{pH} = 5.7$). Each curve demonstrates Langmuir-type behavior. A drastic increase in the amount of R-6G adsorbed ($\Gamma \text{ mol m}^{-2}$) with the SiO_x monolayer coverage is apparent below $2.8 \times 10^{-5} \text{ M}$ of the equilibrium concentration of R-6G (C_{eq}). According to the Langmuir model, Γ can be expressed by the equation of $\Gamma = \Gamma_s \beta C_{\text{eq}} / (1 + \beta C_{\text{eq}})$, where Γ_s is the saturation amount of adsorption and β is K_1/a_1 (K_1 is the equilibrium constant for adsorption process; a_1 is the activity of H_2O in the solution). As shown in the inset, both the plots of $C_{\text{eq}}\Gamma^{-1}$ vs C_{eq} are linear (curve a, $R = 0.987$; curve b, $R = 0.994$). From the slopes and the intercepts at $C_{\text{eq}} = 0$, the adsorption parameters Γ_s and β were determined to be $1.13 \times 10^{-7} \text{ mol m}^{-2}$ and $1.44 \times 10^5 \text{ M}^{-1}$, respectively, for TiO_2 and $2.97 \times 10^{-7} \text{ mol m}^{-2}$ and $3.71 \times 10^5 \text{ M}^{-1}$, respectively, for $\text{SiO}_x/\text{TiO}_2$. These results indicate that the SiO_x monolayer coverage of TiO_2 remarkably increases the adsorption strength

SCHEME 1



SCHEME 2



for R-6G (β) and Γ_s relative to naked TiO_2 . In the previous work, the SiO_x monolayer coverage of TiO_2 was revealed to shift the point of zero charge (pzc) from 7.5 (TiO_2) to 3.2 ($\text{SiO}_x/\text{TiO}_2$) that is near the value for SiO_2 .^{7,9} This fact suggests that a large portion of the TiO_2 surface is covered with the SiO_x monolayer, although the surface coverage could not be determined quantitatively.¹⁰ The increase in the electrostatic attraction between R-6G^+ ions and the surface ($\text{Si}_s\text{-O}^-$) would be responsible for the increases in β and Γ_s . From Γ_s and the area per molecule σ ($1.2 \text{ nm}^2 \text{ molecule}^{-1}$),^{5b} 8.1% (TiO_2) and 21.6% ($\text{SiO}_x/\text{TiO}_2$) of the surfaces were estimated to be covered with R-6G; i.e., the adsorption is limited in a submonolayer region.

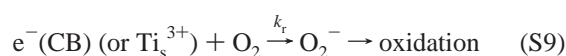
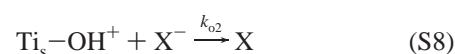
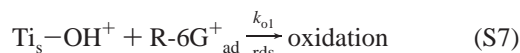
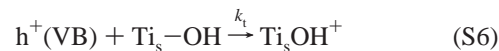
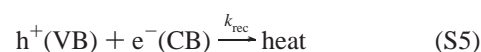
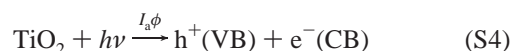
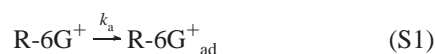
Figure 2A shows electronic absorption spectra of the components in the reaction system. TiO_2 and $\text{SiO}_x/\text{TiO}_2$ have strong absorptions below 385 nm due to the band gap transition (curve a). R-6G has an intense absorption band peaked at 527 nm in the visible range and several bands in the UV range. Then light irradiation ($\lambda > 300 \text{ nm}$) excites both TiO_2 (or $\text{SiO}_x/\text{TiO}_2$) and R-6G. Figure 2B shows time courses of the photoinduced degradation of R-6G ($C_0 \approx 3 \times 10^{-5} \text{ M}$); in these experiments, irradiation ($\lambda > 300 \text{ nm}$) was started after reaching the adsorption equilibrium for each system. Without either TiO_2 (or $\text{SiO}_x/\text{TiO}_2$) (curve r_1) or irradiation (curve r_2), R-6G hardly decomposes in less than 2 h of reaction time. In the presence of TiO_2 (curve a), the concentration significantly decreases with an increase in irradiation time. Noticeably, the degradation rate further increases when $\text{SiO}_x/\text{TiO}_2$ is used as a photocatalyst (curve b).

Two reaction schemes are possible for the light-driven decomposition of R-6G (Schemes 1 and 2). In Scheme 1,¹¹ the electron (e^-) excited from the highest occupied molecular orbital (HOMO, $E_{\text{HOMO}} = -8.95 \text{ eV}$) to the lowest unoccupied molecular orbital (LUMO, $E_{\text{LUMO}} = -1.69 \text{ eV}$) of R-6G^+ is injected into the conduction band (CB) of TiO_2 ($E_{\text{CB}} = -11 \text{ eV}$).¹² Because the LUMO of R-6G^+ is far higher than the CB edge, the electron transfer from the excited R-6G^+ to TiO_2 is thermodynamically allowed. The e^- reduces O_2 adsorbed ($\text{O}_{2\text{ad}}$) on the surface of TiO_2 to yield O_2^- . O_2^- further oxidizes R-6G^{2+} radicals. On the other hand, in Scheme 2, redox reactions are initiated from the band gap excitation of TiO_2 . The hole (h^+) generated in its valence band (VB, $E_{\text{VB}} = -14 \text{ eV}$) oxidizes $\text{R-6G}^+_{\text{ad}}$ after diffusing to the surface. The h^+

transfer from TiO_2 to R-6G^+ is also thermodynamically permitted because the VB edge is lower than the HOMO energy of R-6G^+ . The e^- excited to the CB also participates in the oxidation of R-6G^+ via reduction of $\text{O}_{2\text{ad}}$ in the same manner as in Scheme 1. Visible light ($\lambda > 420 \text{ nm}$) illumination only excites R-6G. Under this condition, no degradation of R-6G was observed in the same range of reaction time (curve c of Figure 2B). It is clear that Scheme 1 can be ruled out and the degradation of R-6G is mainly induced from direct photoexcitation of TiO_2 (or $\text{SiO}_x/\text{TiO}_2$) basically according to Scheme 2. Since the position of the absorption peak at 527 nm was not changed with adsorption, most of light capable of exciting R-6G_{ad} is absorbed by R-6G^+ ions in the bulk solution. This inner filter effect seems to be partly responsible for the fact that no reaction occurred upon visible light illumination.

Figure 3A shows the dependence of the initial rate of R-6G (counteranion, $\text{X} = \text{Cl}^-$) removal from the solution (v_0) on its initial concentration (C_0); in these experiments, irradiation was started just after dispersing the photocatalysts into the reaction solutions. In each case (curve a, TiO_2 ; curve b, $\text{SiO}_x/\text{TiO}_2$), v_0 increases monotonically with increasing C_0 . When compared at the same C_0 , the value of v_0 for $\text{SiO}_x/\text{TiO}_2$ is greater than for TiO_2 over the whole range of C_0 tested ($1 \times 10^{-6} < C_0 < 1 \times 10^{-5} \text{ M}$). A plausible reaction mechanism on the TiO_2 (or $\text{SiO}_x/\text{TiO}_2$) photoinduced degradation of R-6G is presented in Scheme 3.

SCHEME 3



In the usual LH kinetics, the value of θ at the equilibrium state under dark conditions is approximately adopted and the following equation is obtained:¹³

$$\frac{1}{v_0} = \frac{1}{k_L} + \frac{1}{k_L K C_0}, \quad (k_L \ll k_a C) \quad (\text{1})$$

where k_L is the apparent rate constant of photodecomposition, k_a is the rate constant of adsorption (min^{-1}), and K is the equilibrium constant of R-6G adsorption.

It should be noted that this formulation is strictly valid only when $k_L \ll k_a C$. However, in separate experiments on the rate of adsorption, $k_L/(k_a C)$ is estimated to be above unity in the concentration range below $3 \times 10^{-5} \text{ M}$ for both the TiO_2 and $\text{SiO}_x/\text{TiO}_2$ systems (data not shown). Then the removal of R-6G^+ ions from the solution was assumed to be accomplished

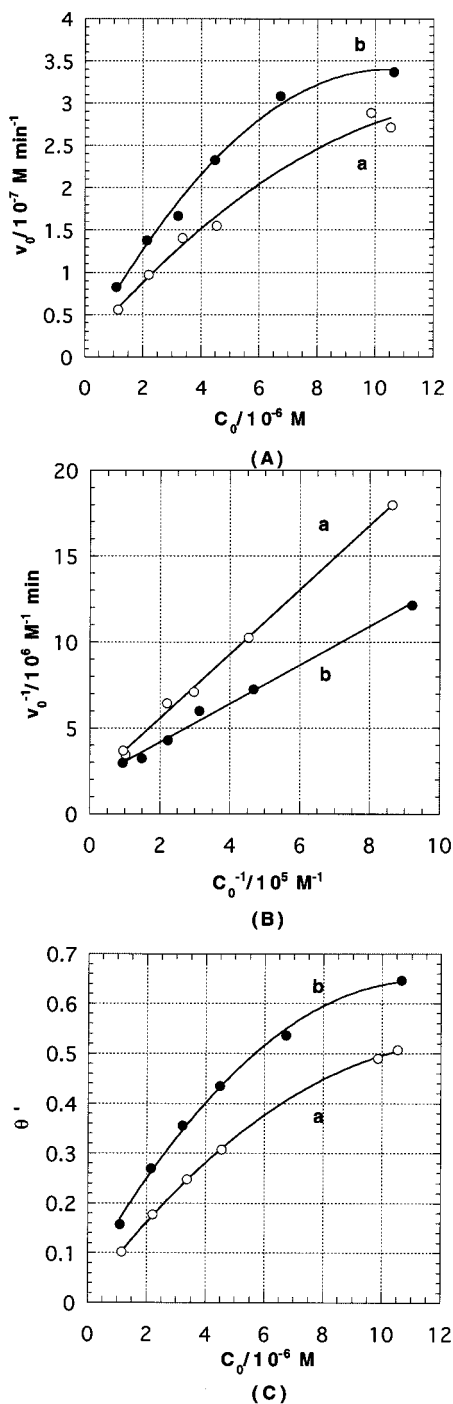


Figure 3. (A) Initial rates of R-6G ($X = \text{Cl}^-$) removal from the solution (v_0) as a function of initial concentrations (C_0) for TiO_2 (a) and $\text{SiO}_x/\text{TiO}_2$ (b) systems. In these experiments, irradiation was started just after dispersing the photocatalysts into the reaction solutions. (B) Plots of v_0^{-1} vs C_0^{-1} for TiO_2 (a) and $\text{SiO}_x/\text{TiO}_2$ (b) systems. (C) Dependence of coverage (θ') on C_0 for TiO_2 (a) and $\text{SiO}_x/\text{TiO}_2$ (b) systems. The coverages at the initial stage of the reaction was calculated from k_a , k_L , and C_0 using eq 1.

with adsorption followed by the photocatalytic decomposition before desorption. This would be a good approximation for the dilute reaction systems containing reactants with large β values. The rate of adsorption (v_a) is expressed by $v_a = -dC/dt = k_a C(1 - \theta')$, where $\theta' (< \theta)$ is the coverage of R-6G⁺ ($=\Gamma/\Gamma_s$), and is *not for dark conditions but for the photostationary state*. The lifetime of h^+ ranges from 10^{-19} to 10^{-3} s and the diffusion time across the space charge region in n-TiO₂ was calculated to be on the order of 10^{-14} s.^{13a} Thus, the

surface, upon illumination, will come rapidly to an active steady state including h^+ . Since θ' is determined by the balance between v_a and the rate of decomposition written as $k_L \theta'$, the equation of $\theta' = k_a C / (k_L + k_a C)$ is derived. Substituting this expression for θ' in the differential equation, one can obtain eq 2 relating C_0 to v_0 at the initial stage of the reaction:

$$\frac{1}{v_0} = \frac{1}{k_L} + \frac{1}{k_a C_0} \quad (k_L \geq k_a C) \quad (2)$$

In a limiting case ($k_L \gg k_a C$), the rate of the reaction is completely controlled by the diffusion process and eq 2 is reduced to eq 3:

$$v_0 = k_a C_0, \quad (k_L \gg k_a C \text{ and } \theta' \approx 0) \quad (3)$$

As shown in Figure 3B, plots of v_0^{-1} vs C_0^{-1} for both systems yield straight lines (curve a, $R = 0.999$; curve b, $R = 0.996$). From the slopes and intercepts, the values of k_a and k_L for $X = \text{Cl}^-$ were calculated to be 0.053 min^{-1} and $5.4 \times 10^{-7} \text{ M min}^{-1}$, respectively, for TiO_2 and 0.089 min^{-1} and $5.2 \times 10^{-7} \text{ M min}^{-1}$, respectively, for $\text{SiO}_x/\text{TiO}_2$. The rate of R-6G⁺ adsorption increases by a factor of 1.7 with the SiO_x monolayer coating, while the rate of the photodecomposition on the surface remains almost constant. A similar result was obtained in the system of CPB.⁷

Figure 4A shows plots of v_0 vs C_0 for R-6G ($X = \text{NO}_3^-$). The v_0 increases with increasing C_0 in each case (curve a, TiO_2 ; curve b, $\text{SiO}_x/\text{TiO}_2$). The accelerating effect of the SiO_x monolayer coverage is further enhanced compared with the system of $X = \text{Cl}^-$, whereas the value of v_0 is smaller. Plots of v_0^{-1} vs C_0^{-1} give two straight lines also in these cases (Figure 4B). From the same analysis described above, the values of k_a and k_L for $X = \text{NO}_3^-$ were obtained to be 0.036 min^{-1} and $1.23 \times 10^{-7} \text{ M min}^{-1}$, respectively, for TiO_2 and 0.095 min^{-1} and $3.39 \times 10^{-7} \text{ M min}^{-1}$, respectively, for $\text{SiO}_x/\text{TiO}_2$. When $X = \text{NO}_3^-$, k_a and k_L are increased remarkably with the SiO_x monolayer coverage. Figures 3C and 4C show θ' values calculated from the k_a and k_L values as a function of C_0 . Clearly, $k_a C$ are comparable to k_L under the present experimental conditions; this also substantiates the validity of the kinetic analyses using eq 2.

Taking into account only the concentration gradient as the driving force of the diffusion for the TiO_2 system, one can obtain eq 4:

$$k_a = -\frac{1}{C_0} \left(\frac{dC}{dt} \right)_0 = -\frac{1}{C_0} \left(\frac{JS}{v} \right)_0 \quad (4)$$

where J is the flux of R-6G from the bulk solution to the surface, S is the active surface area, and v is the volume of the reaction suspension. Since $J = -D(dC/dx)_0$,

$$k_a = \frac{DS(dC/dx)_0}{C_0 v} = \frac{DS}{v \delta x} \quad (5)$$

where D is the diffusion coefficient of R-6G and δx is the thickness of the diffusion layer.

The absorption length of the TiO_2 suspension was calculated to be ca. 0.8 cm using the absorption coefficient of TiO_2 ($\alpha \approx 5 \times 10^4 \text{ cm}^{-1}$) and the volume fraction of the particles in the suspension (2.6×10^{-5}). Since the depth of the suspension in the direction of incident light is 8 cm, the value of S was estimated to be 400 cm^2 from BET surface area \times (0.8 cm/8 cm). Substitution of appropriate numerical values ($D = 2 \times$

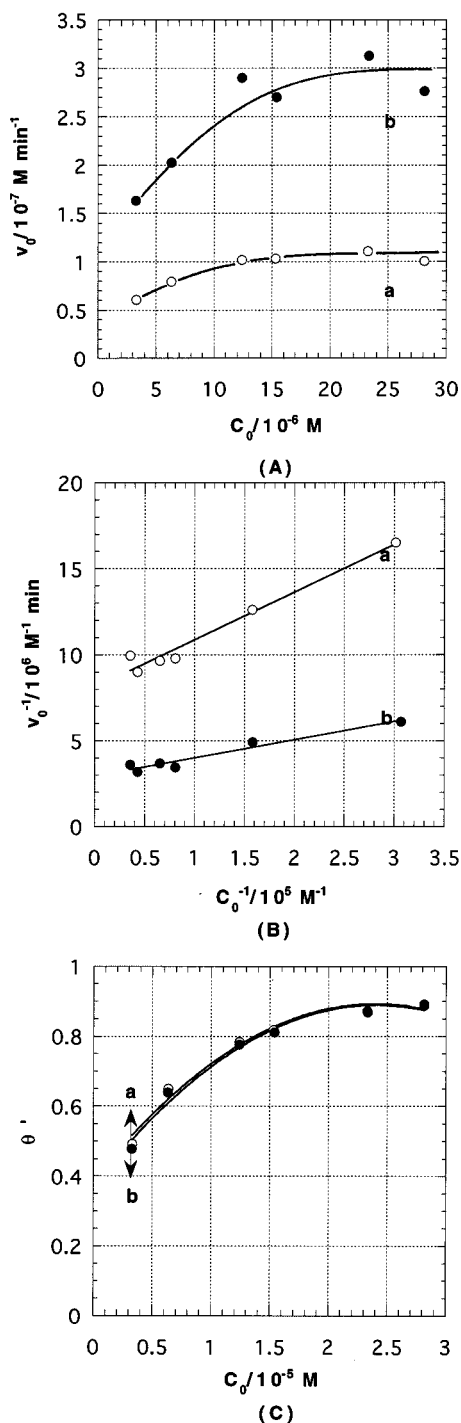


Figure 4. (A) Plots of v_0 vs C_0 for TiO_2 (a) and $\text{SiO}_x/\text{TiO}_2$ (b) systems ($X = \text{NO}_3^-$). In these experiments, irradiation was started just after dispersing the photocatalysts into the reaction solutions. (B) Plots of v_0^{-1} vs C_0^{-1} for TiO_2 (a) and $\text{SiO}_x/\text{TiO}_2$ (b) systems. (C) Dependence of θ' on C_0 for TiO_2 (a) and $\text{SiO}_x/\text{TiO}_2$ (b) systems.

$10^{-6} \text{ cm}^2 \text{ s}^{-1}$,¹⁴ $v = 50 \text{ cm}^3$, $\delta x = 0.05 \text{ cm}$,¹⁵ $S = 400 \text{ cm}^2$) into eq 5 yields a k_a value of 0.02 min^{-1} , which is in good agreement with the experimental values for the TiO_2 systems.

The gas-phase photodecomposition of R-6G adsorbed on TiO_2 (a) and $\text{SiO}_x/\text{TiO}_2$ (b) in the air was studied. This reaction is quite different from the liquid-phase one in that it does not involve the diffusion process of R-6G. In each absorption spectrum, an absorption band and a shoulder, respectively due to R-6G monomers and dimers, are observed at 528 and 490 nm (data not shown).¹⁶ Upon irradiation ($\lambda > 300 \text{ nm}$), their

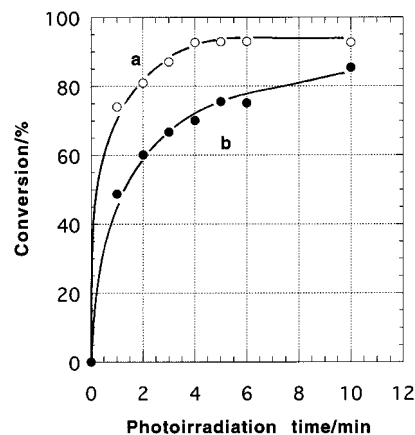


Figure 5. Conversions of R-6G adsorbed on TiO_2 (a) and $\text{SiO}_x/\text{TiO}_2$ (b) as a function of illumination time. Photoillumination ($\lambda > 300 \text{ nm}$) was carried out in the air.

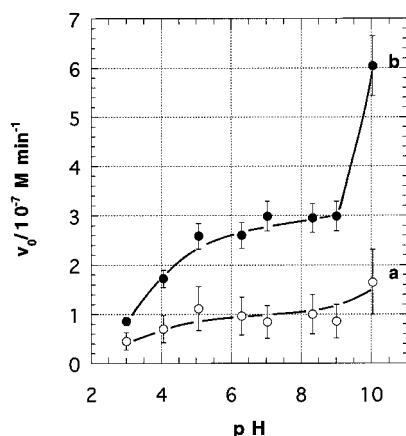
intensities decline with increasing time. Figure 5 shows conversions of R-6G as a function of illumination time; the conversion was calculated from the variation of the absorbance at 528 nm. The rate constants of the photodecomposition (k_{G1}) for TiO_2 and $\text{SiO}_x/\text{TiO}_2$ systems were determined to be 2.6 ± 0.2 and $1.05 \pm 0.05 \text{ min}^{-1}$, respectively, by applying the first-order rate equation.^{5b} A similar retarding effect of the SiO_x monolayer coating was also observed in the gas-phase photo-induced oxidation of the TMCTS monolayer chemisorbed on TiO_2 films ($k_{G2}(\text{TiO}_2) = 0.013 \text{ min}^{-1}$, $k_{G2}(\text{SiO}_x/\text{TiO}_2) = 0.005 \text{ min}^{-1}$).^{6b}

The kinetic parameters for the liquid-phase and gas-phase reactions are summarized in Table 1. First, in the liquid-phase reaction, k_a is as much as 1.7 ($X = \text{Cl}^-$) and 2.6 ($X = \text{NO}_3^-$) times increased by coating TiO_2 with the SiO_x monolayer. This fact is attributable to the 2.6-fold increase in β due to the electrostatic attraction between R-6G^+ and the surface (Si_s-O^-). As anticipated from eq 2, the contribution of the increase in k_a to the increase in v_0 becomes greater with decreasing concentration of R-6G (Figures 3B and 4B). This finding means that the effect of the SiO_x monolayer coverage is emphasized as the concentration decreases, which is of great importance in the practical water purification using TiO_2 photocatalysts. Practically, the concentration of water contaminants lies in the range from ppb to ppm levels. Figure 6 shows the dependence of v_0 on the pH of the solution for TiO_2 (a) and $\text{SiO}_x/\text{TiO}_2$ (b) systems ($X = \text{Cl}^-$). In each system, v_0 increases with increasing pH, i.e., with decreasing amount of the surface positive charge or increasing amount of the surface negative charge. A remarkable increase in v_0 with the SiO_x monolayer coverage is observed over the whole pH range tested ($3 < \text{pH} < 10$). However, the difference in v_0 between systems a and b decreases as the pH approaches the pzc value of the $\text{SiO}_x/\text{TiO}_2$ particles (3.2). This result again points to the significance in the electrostatic interaction between R-6G^+ and the surface of the photocatalyst. It should also be noted that the increase in v_0 with increasing pH in system a is much smaller than that with the SiO_x monolayer coating.

The second striking point is that the k_L value for $\text{SiO}_x/\text{TiO}_2$ is comparable to ($X = \text{Cl}^-$) or 2.8-fold greater ($X = \text{NO}_3^-$) than for TiO_2 , while k_{G1} and k_{G2} decrease with the SiO_x monolayer coating by a factor of 0.4. Because the SiO_x monolayer has no absorption for $\lambda > 300 \text{ nm}$, the photon quantity absorbed by TiO_2 is invariant with its coating. The inhibition of the interfacial charge transfer by the SiO_x insulating monolayer, i.e., decrease in k_{o1} in Scheme 3, may be responsible

TABLE 1: Comparison of Kinetic Parameters in the TiO₂- and SiO_x/TiO₂-Photoinduced Decomposition of R-6G

X	liquid phase				gas phase			
	k_a (min ⁻¹)		k_L (M min ⁻¹)		k_{G1} (min ⁻¹)		k_{G2} (min ⁻¹)	
	TiO ₂	SiO _x /TiO ₂	TiO ₂	SiO _x /TiO ₂	TiO ₂	SiO _x /TiO ₂	TiO ₂	SiO _x /TiO ₂
Cl ⁻	0.053	0.089	5.43×10^{-7}	5.18×10^{-7}	2.6 ± 0.2	1.05 ± 0.005	0.013	0.005
NO ₃ ⁻	0.036	0.095	1.23×10^{-7}	3.39×10^{-7}				

**Figure 6.** Dependence of v_0 on the pH of the solution for TiO₂ (a) and SiO_x/TiO₂ (b) systems ($X = \text{Cl}^-$). In these experiments, irradiation was started just after dispersing the photocatalysts into the reaction solution. The initial concentration was fixed at 5×10^{-6} M.

for the decrease in k_G . An exponential decrease in the reaction rate with increasing SiO_x film thickness was observed in the gas-phase oxidation of the chemisorbed TMCTS monolayer.^{6b} The fact suggests that the oxidation is limited by the formation rate of oxidants on the surface via tunneling of photogenerated charge carriers through the SiO_x film, although further experiments are necessary to specify the active surface oxidant species.¹⁷ Since this seems to be true also for the liquid-phase reaction (decreases in k_{o1} and k_{o2}), a mode of action for improving the reaction efficiency, which is unique in the liquid-phase reaction, must be taken into account to explain the fact of $k_L(\text{SiO}_x/\text{TiO}_2) \geq k_L(\text{TiO}_2)$. In Scheme 3, if step 7 is presumed to be the rate-determining step (rds) of the photoinduced decomposition of R-6G, eq 6 is obtained by applying the steady-state approximation to $[\text{Ti}_s\text{-OH}^+]$ and $[\text{h}^+]$ for a low light intensity condition,

$$k_L = \frac{I_a \phi k_{o1}}{k_{o1} \theta + k_{o2} \frac{[\text{X}^-_{\text{ad}}]}{[\text{R-6G}^+_{\text{ad}}]_s}} \quad (6)$$

where $[\text{R-6G}^+_{\text{ad}}]_s$ is the saturated adsorption concentration of R-6G.

For simplicity, the adsorption sites for R-6G⁺ and X⁻ were assumed to be different and mutually independent in the derivation. Since $\theta(\text{SiO}_x/\text{TiO}_2) \geq \theta(\text{TiO}_2)$ (Figures 3C and 4C), the increase in k_L would result from the second term in the denominator. The 2.6-fold increase in $[\text{R-6G}^+_{\text{ad}}]_s$ or Γ_s is confirmed in the adsorption experiments (Figure 1), indicating the increase in the number of adsorption sites ($\text{Si}_s\text{-O}^-$). Also, Matthews et al. reported that some anions suppress the rate of the photocatalytic oxidation of organics in aqueous solutions.¹⁸ Also, Schwartz et al. have more recently confirmed, using the electron paramagnetic resonance technique, that the concentration of OH radicals in illuminated TiO₂ suspensions is decreased in the presence of various anions.¹⁹ These facts were accounted for by the participation of the anions in the redox reaction as

an h⁺ or OH radical ($\text{Ti}_s\text{-OH}^+$) scavenger. It is suggested that h⁺ or Ti_sOH^+ is consumed by the oxidation of both R-6G⁺ and X⁻ in the case of TiO₂, while R-6G⁺ is predominantly oxidized in the case of SiO_x/TiO₂ because of anion exclusion from the surface due to the electrostatic repulsion between X⁻ and $\text{Si}_s\text{-O}^-$ (decrease of $[\text{X}^-_{\text{ad}}]$ in eq 2). Consequently, the increase in k_L with the SiO_x monolayer coverage is rationalized in terms of the increase in $[\text{R-6G}^+_{\text{ad}}]_s$ and/or decrease in $[\text{X}^-_{\text{ad}}]$. According to Herrmann and Pichat, because Cl⁻ ions can withstand the TiO₂ photocatalytic oxidation,²⁰ the large gap in k_L between the substrates with different anions may be associated with anion oxidizability and/or adsorbability ($[\text{X}^-_{\text{ad}}]$) of anions. However, further studies are necessary to draw this conclusion.

Conclusions

The effect of coating TiO₂ with the SiO_x monolayer on the photoinduced oxidation of R-6G in aqueous solutions was studied. Adsorption experiments showed that the surface treatment significantly increases the saturated adsorption amount and the adsorption strength of R-6G. It was further demonstrated that the liquid-phase oxidation of R-6G is remarkably enhanced with the treatment, whereas it suppresses the gas-phase reaction. A modified Langmuir–Hinshelwood mechanism was proposed, explaining the promoting effect in the liquid-phase reaction in terms of the increases in the rate of adsorption, the saturation amount of adsorption, and/or the decrease in the adsorption amount of anions. This work exhibits high validity of oxide monolayer coverage in purifying water-containing ionic contaminants using TiO₂ photocatalysts. The key is to increase the rate of adsorption without decreasing the rate of decomposition on the surface. This methodology is going to be developed to accelerate photooxidation of anionic substrates in our laboratory.

Acknowledgment. The authors express sincere gratitude to Ishihara Techno Co. for the gift of the TiO₂ particles (A-100) and to Dr. M. Iwasaki of Kinki University for valuable comments.

References and Notes

- (1) In *Photocatalytic Purification and Treatment of Water and Air*; Ollis, F. D., Al-Ekabi, H., Eds.; Elsevier Science: Amsterdam, 1993.
- (2) Hoffmann, M. R.; Martin, S. T.; Choi, W.; Bahnemann, D. W. *Chem. Rev.* **1995**, *95*, 69.
- (3) (a) Tada, H.; Tanaka, M. *Langmuir* **1997**, *13*, 360. (b) Hattori, A.; Tada, H.; Yamamoto, M.; Ito, S. *Chem. Lett.*, in press.
- (4) (a) Sampath, S.; Uchida, H.; Yoneyama, H. *J. Catal.* **1994**, *149*, 189. (b) Anderson, C.; Bard, A. J. *J. Phys. Chem.* **1995**, *99*, 9882. (c) Anderson, C.; Bard, A. J. *J. Phys. Chem. B* **1997**, *101*, 2611.
- (5) (a) Tada, H. *Langmuir* **1995**, *11*, 3281. (b) Tada, H. *Langmuir* **1996**, *12*, 966.
- (6) (a) Tada, H.; Kubo, Y.; Akazawa, M.; Ito, S. *Langmuir* **1998**, *14*, 2936.

- (8) Dewar, M. J. S.; Zuebisch, E. G.; Healy, E. F.; Stewart, J. J. P. *J. Am. Chem. Soc.* **1985**, *107*, 3902.
- (9) Odenbrand, C. V. I.; Bransin, J. G. M.; Busca, G. J. *Catal.* **1992**, *135*, 505.
- (10) In the SiO_x monolayer formed on plain TiO₂ films, the thickness of the SiO_x layer (*d*) was confirmed by ellipsometry to increase in proportion to the coating times (*n*). Also, the slope of the plot of *d* vs *n* provided a value of ca. 0.2 nm/time, which corresponds to the thickness of the SiO₂ monolayer. For details, see ref 6a.
- (11) Kamat, P. V. *Chem. Rev.* **1993**, *93*, 267.
- (12) The VB and CB energy levels were adopted from the following literature. Hoffmann, R. *A Chemist's View of Bonding in Extended Structures*; VCH Publishers: New York, 1993.
- (13) (a) Pruden, A. L.; Ollis, D. F. *J. Catal.* **1983**, *82*, 404. (b) Ohtani, B.; Okugawa, Y.; Nishimoto, S.-i.; Kagiya, T. *J. Phys. Chem.* **1987**, *91*, 3550. (c) Matthews, R. W. *J. Chem. Soc., Faraday Trans. 1* **1989**, *85*, 1291. (d) Cunningham, J.; Al-Sayyed, G. *J. Chem. Soc., Faraday Trans.* **1990**, *86*, 3935.
- (14) Glasstone, S.; Laidler, K. J.; Eyring, H. *The Theory of Rate Processes*; McGraw-Hill, Inc.: New York, 1964.
- (15) Bockris, J. O'M.; Reddy, A. K. N. *Modern Electrochemistry*; Plenum Press: New York, 1970.
- (16) Hayakawa, K.; Satake, I.; Kwak, J. C. T.; Gao, Z. *Colloids Surf.* **1990**, *50*, 309.
- (17) Fox, M. A.; Dulay, M. T. *Chem. Rev.* **1993**, *93*, 341.
- (18) Abdullah, M.; Low, G. K.-C.; Matthews, R. W. *J. Phys. Chem.* **1990**, *94*, 6820.
- (19) Schwarz, P. F.; Turro, N. J.; Bossmann, S. H.; Braun, A. M.; Wahab, A.-M. A. A.; Durr, H. *J. Phys. Chem. B* **1997**, *101*, 7127.
- (20) Herrmann, J.-M.; Pichat, P. *J. Chem. Soc., Faraday Trans. 1*, **1980**, *76*, 1138.